Feasibility Study of Using UAVs as GNSS Satellites

Daniel S. Maier, Thomas Kraus, Ronny Blum, Mathias Philips-Blum, Thomas Pany,
Universität der Bundeswehr München, Institute of Space Technology and Space Applications, 85577 Neubiberg, Germany

BIOGRAPHIES

Daniel S. Maier has a professional training as a technical draftsman and received his master in Applied and Engineering Physics from the Technical University of Munich (TUM), Germany. Since 2017 he is a research associate at the University of Federal Armed Forces Munich at the Institute of Space Technology and Space Applications. His current research interests include GNSS signal performance analysis.

Thomas Kraus graduated with a M.Sc. in Electrical Engineering from the University of Darmstadt, Germany. In 2008, he joined the Institute of Space Technology and Space Applications of the "Universität der Bundeswehr München". He's been working as a research associate on several projects of the German Space Agency (DLR) and European Space Agency (ESA-ESTEC). His main research focus is on future receiver design offering a superior detection and mitigation capability of intentional and unintentional interferences.

Ronny Blum received his master in Physics from the University of Basel, Switzerland. Since then he worked at Würth Elektronik in the field of signal transmission and later on at the Forest Research Institute in Freiburg im Breisgau in the field of GNSS reception within the forest. 2017 he joined the University of Federal Armed Forces Munich, where he is working in the field of GNSS software receiver.

Mathias Philips-Blum received his master in Geodesy and Geoinformatics from the Leibniz University of Hannover, Germany. Since 2017 he is a research associate at the University of Federal Armed Forces Munich at the Institute of Space Technology and Space Applications. He currently works in the field of sensor fusion and navigation.

Prof. Thomas Pany is with the Universität der Bundeswehr München at the faculty of aerospace engineering where he teaches satellite navigation. His research includes all aspects of navigation ranging from deep space navigation over new algorithms and assembly code optimization. Currently he focuses on GNSS signal processing for Galileo second generation, GNSS receiver design and GNSS/INS/LiDAR/camera fusion. To support this activities, he is developing a modular GNSS test bed for advanced navigation research. Previously he worked for IFEN GmbH and IGASPIN GmbH and is the architect of the ipexSR and SX3 software receiver. He has around 200 publications including patents and one monography.

ABSTRACT

The upcoming challenges on GNSS regarding spoofing, jamming, multipath, and interference, also from multi-constellations, require a detailed analysis on the GNSS signal level. Therefore, a testing method is needed which goes beyond the possibilities of simulations to create a realistic and flexible test environment. The progress in unmanned aerial vehicles (UAV) and software defined radio (SDR) technologies obtained in the last years provide this efficient and flexible approach to mimic GNSS satellites and create a realistic GNSS signal test environment.

Within this work we present our experience in setting up a flying test system. Beside UAV and SDR our system includes a positioning and ranging unit to obtain the transmitter-receiver ranges in sub-centimeter and millisecond timestamp accuracy. To eliminate the UAV clock error, two time synchronized receiver units are used. In this first feasibility step we concentrate on a single BPSK(1) on 1576.17 MHz signal and show that the USRP 2950R (NI) can operate in a standalone mode, generating the signal on the FPGA, which is driven by the OCXO onboard clock. It is presented that the recorded Doppler shift represents the UAV motion as well as that the phase pseudorange difference of two antennas can be well (7 cm RMS) matched to the geometrical antenna-UAV range difference (cancelation of the SDR clock error).

It is shown that the combination of UAV and SDR can be used to mimic a GNSS satellite. Therefore, it is possible to use this arrangement for realistic GNSS signal analyses under various conditions, environments and disturbances.

INTRODUCTION

There is an increasing importance of GNSS open services for our economy, society and security e.g. in the field of traffic monitoring and controlling be it in the air, on see or at land, or in first aid response in any kind of emergency, as well as for timing applications like bank transactions or power grid synchronization. Due to this developments it is necessary to enhance the availability and more important the reliability of the GNSS service. Improving the signal robustness against multipath, jamming, spoofing and interference from secondary sources or even other constellations is a crucial task for the future research and development. To improve the GNSS signals one has to test and analyze the signals under various conditions. This was and is done manly with computer simulations. These simulations are easy and cheap to realize as well as flexible and repeatable. However, a simulation relies always on assumptions and simplifications of a real world problem. Therefore, we develop a flexible, cost efficient and highly adjustable test system, usable for real test scenarios. With this system, we can investigate the GNSS signal structures, authentication methods, channel coding and signal behavior under jamming, spoofing and other interferences. In the first part we explain the concept of the system followed by a description of the necessary components. In the end the first results and the conclusion for future developments is presented.

CONCEPT

A UAV with a software defined radio (SDR) on board is used as a pseudo satellite. Two patch antennas were positioned on the ground with a distance of around 12.5 meters apart from each other. The antennas are connected to one software receiver, which is able to track both signals in parallel. The two incoming signals are both tracked and processed with the same receiver clock and receiver clock error. With the two antennas it is possible to eliminate the clock error from the SDR (dt_{sv}) and the software receiver (dt_r). Equation 1 and 2 give the measured pseudoranges for the antennas one and two. Subtracting the observed pseudoranges $P_1 - P_2$ leads to equation 3 which is independent of the clock errors dt_r and dt_{sv}. If the geometrical range difference $\Delta GR = \rho_1 - \rho_2$ is known, it is possible to investigate the error difference $\varepsilon_1 - \varepsilon_2$. The influence of multipath, jamming, spoofing and other interferences on the signal can be studied. The ionosphere and troposphere error do not have a significant influence since the distance from drone to antenna is small. The absolute pseudorange is in our case of no importance because we only investigate the pseudorange difference. An identical pseudorange offset in both pseudoranges has no influence on the evaluation and is cancelled out in the difference.

$$P_1 = \rho + c\,(dt_{sv} - dt_r) + \varepsilon_1 \qquad (1)$$

$$P_2 = \rho_2 + c\,(dt_{sv} - dt_r) + \varepsilon_2 \qquad (2)$$

$$P_1 - P_2 = \rho_1 - \rho_2 + \varepsilon_1 - \varepsilon_2 \qquad (3)$$

P_1: Pseudorange from antenna 1 to drone
P_2: Pseudorange from antenna 2 to drone
ρ_1: Real distance from antenna 1 to drone
ρ_2: Real distance from antenna 2 to drone
c: Speed of light
dt_{sv}: Clock error SDR
dt_r: Clock error receiver
ε_1: Residual PR error from antenna 1 to drone
ε_2: Residual PR error from antenna 2 to drone

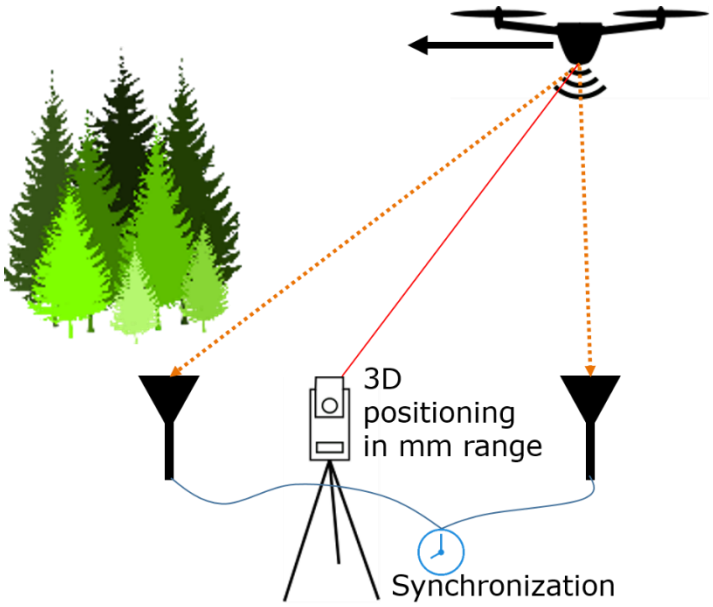

Figure 1: Concept sketch of the measurement setup.

The difference of the measured pseudoranges only contains the geometrical range difference and a remaining residual error $\varepsilon_1 - \varepsilon_2$. This error comes mainly from multipath, but also receiver noise, tracking delay and noise from the electronic. One idea of our measurement setup is to influence the line of sight from one antenna by multipath and leave the other line of sight unobscured. Therefore ε_1 changes differently than ε_2 and $\varepsilon_1 - \varepsilon_2$ is directly related to the influence of multipath on the signal. To get $\varepsilon_1 - \varepsilon_2$, the real distance from the antennas to the drone (ρ_1, ρ_2) has to be known. This is measured with a tacheometer,

which can determine the coordinates of the drone and the antennas with millimeter accuracy. The used tacheometer is able to follow the drone, which allows static and kinematic measurements.

COMPONENTS

There are four relevant components if one want to use UAV's as GNSS satellites and performing signal analysis: The transmitter and receiver systems which have to be tuned to achieve the desired results, the positioning and ranging system which is used for precise position measurements of the antennas and the UAV, as well as the UAV itself which has to carry the payload. This section gives a detailed description of the used components in the used setup and some performance details.

Transmitter/Receiver

The most relevant part on the transmitter site is the clock. Therefore the clock characteristics where tested and evaluated for the use as GNSS signal transmitter. The National Instruments (NI) devices USRP 2920 [3] and USRP 2950R [1][2] were probed for usage. In both SDR's is a TCXO with a frequency accuracy of $\pm$2.5E-6. The USRP 2950R has an additional OCXO (GPS mode) with a frequency accuracy of $\pm$25E-9 (not locked to GPS). As the TXCO is equal in both devices we will only show the results for the USRP 2950R in the following. The internal USRP 2950R clocks were compared with the Symmetricom XPRO Rubidium Oscillator [4] with a frequency accuracy of $\pm$5E-11. The generation of the spreading code as well as the controlling of the USRP was realized with a LabVIEW program. The program generates the GPS PRN-code and upsamples it to 10.23 MHz, afterwards it is downsampled to the final bandwidth of 4MHz, to match it to the maximum data rate of the used 'Express Card' slot, and repeated in real time. Per queuing function the data stream is sent to the USRP where it is upconverted to the final carrier frequency of $f_{L1} = 1576{,}42$ MHz. The HF signal was transmitted via coax cable to the IFEN NavPort front-end and recorded and analyzed with the IFEN SX3 GNSS Software. In Figure 2 the results for the Doppler shift analysis of all three clocks is presented. At the top, the USRP2950R internal TCXO is used. It is clearly visible that the clock stability is not sufficient to hold the phase lock over a larger period of time. In the middle, the Doppler shift using the internal USRP2950R OCXO is plotted. Even if the OCXO is not locked to GPS, the stability is acceptable for the GNSS signal transmitting purpose. The offset of approximate -580 Hz is no issue for the later studies. At the bottom, the XPRO Rubidium Oscillator performance is displayed. A smaller Doppler offset is visible, otherwise the performance in stability is comparable to the OCXO.

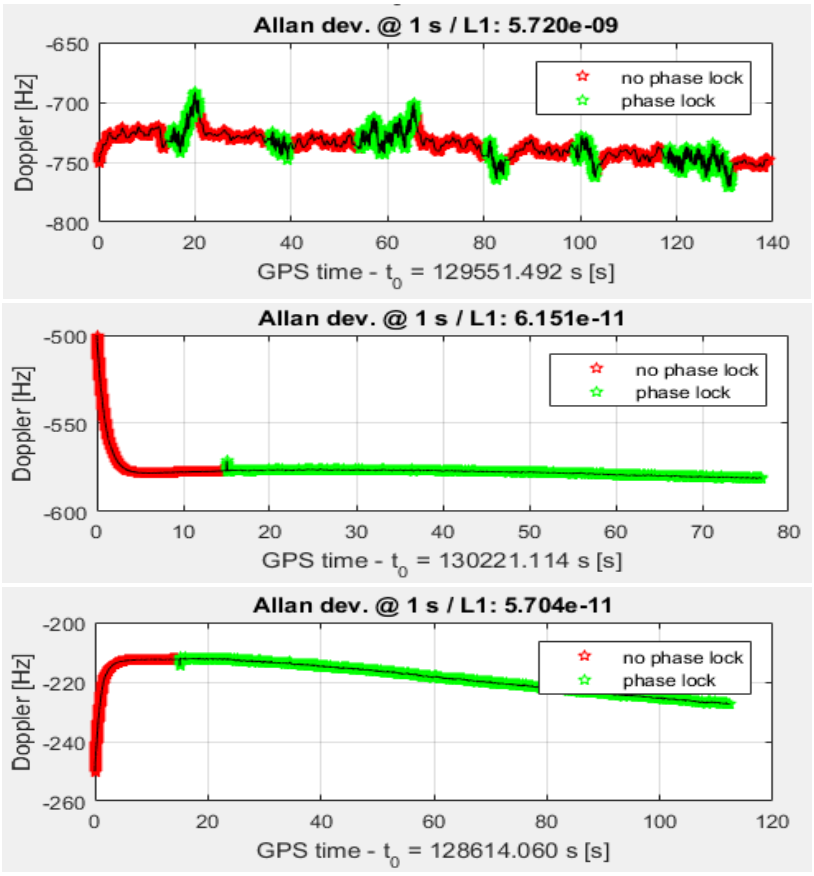

Figure 2: Doppler shifts for three different clocks. Top: USRP2950R intern TCXO; Middle: USRP2950R intern OCXO; Bottom: Extern Atomic Rubidium Oscillator.

After verifying the usability of the USRP 2950R for the desired purpose the spreading code generation and sampling step was implemented on the USRP internal FPGA Xilinx Kintex 7. The FPGA implementation must be adapted to the hardware of an FPGA. That is why we are limited in the way of implementation. The concept for the FPGA-firmware is illustrated in Figure 3. The first block is a Square Wave Generator as NCO, which is part of the NI LabVIEW library. An Edge Detector provides one pulse for a following counter. This counter runs from 0 to 1022, which is the address for the Look-Up-Table (LUT) containing the PRN code. Finally, the native code of NI will be used for upconversion and transmission.

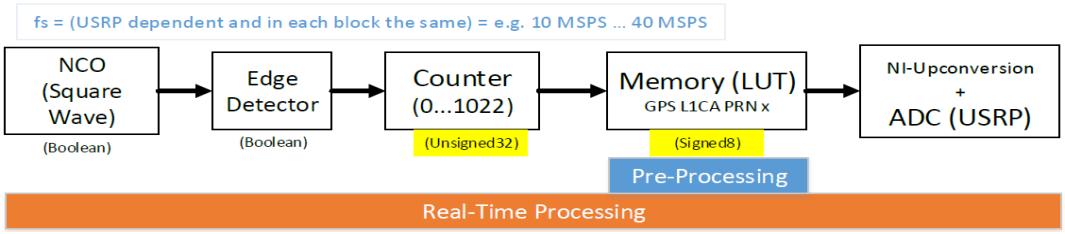

Figure 3: The FPGA dataflow chart.

As the signal generation is internal and also the internal clock can be used, it was favored to run the USRP in a standalone mode and not using an external CPU for controlling. However, the hardware is not supposed to be used standalone. But we were able to overcome this limitation with a small hardware based disconnection procedure. This procedure works only by using a Laptop with 'Express Card' slot, a NI ExpressCard-8360 and the ExpressCard MXI Cable connecting the laptop with the USRP. If the PC and the USRP are connected in this way it is possible to start the FPGA program and unplug the ExpressCard afterwards, without stopping the program. The energy support for the USRP is realized with a battery pack.

On the receiver side we were using the IFEN SX3 Dual-RF Multi-GNSS Software Receiver Front-end [5]. With the Dual-RF Front-end the recorded signals of both antennas are time synchronized and can be used for post processing without additional effort. Two Trimble Zephyr 2 Geodetic antennas are used for the first measurements. A frequency offset of 750 kHz was applied, so the used carrier frequency was 1.57617 GHz (1.57542 GHz + 750 kHz). With this offset we can operate the system without influencing the GPS service in the surrounding area.

As mentioned before the transmitted signal is without data bits and therefore without any time information. To overcome this lack of information in the pseudorange determination the Hardsync option was used in the software receiver. This option sets a specific time stamp to the recording start. This procedure can be used and is uncritical as we are only interested in the pseudorange differences and therefore all constant time offsets are canceled.

Positioning and Ranging

For the positioning and ranging the Leica "Nova MS60 MultiStation" [6] is used. The tacheometer uses the reflection of a mirror for a time of flight measurement and the corresponding angular information for the ranging and positioning. The accuracy for the horizontal and vertical angle as well as the ranging for the MS60 MultiStation is given in Table 1.

Table 1: The measurement accuracy for the Leica MS60 MultiStation. The ppm (parts per million) contribution is distance depending.

	Angle		Range
Total Station	$\sigma_{horizontal}$ ["]	$\sigma_{vertical}$ [°]	σ_{range} [mm]
MS 60	1	0,9	2mm +2,5ppm

The UAV coordinate computation was done in post-processing. The necessary measurement data include horizontal angle, vertical angle, distance and internal time stamp. In the setup we were using the features of autonomous tracking. Therefore, the Leica 360°-Miniprism (GRZ101) [7] is used, compare Figure 5. The Miniprism allows a direction independent (360°) tracking and do not raise the payload weight significantly. The autonomous tracking-mode of the system enables a persecution of the prism up to a distance of 250 m. Due to the Piezo-Engines, the MS 60 is able to follow the reflector movements with a tracking speed up to 14 m/s. If the reflection of the prism is lost, the MS60 can retrieve the prism location with a method called "Power Search". This method works sufficiently while the drone hovers. From the given accuracy of the MS 60, mentioned above, an uncertainty for the position can be derived. In the case of the maximum tracking distance of the system (250 m), the uncertainty in measurement direction (northing) is ± 1 mm. The uncertainty crosswise to the measurement direction and for the height is ± 1.2 mm (easting, Height).

The coordinate system is determined by recording the direction angle to one known point in the local system and fix it as the reference angle. This reference axis corresponds to the direction of the x-axis (northing). All measurements to the drone, which are done for the measurement campaign from now, are all corrected by this reference direction. By using the determined angles and distances the 3D coordinates of the drone are computed via trigonometric functions. This method is called "Polar point determination", compare Figure 4. The antenna phase center position is calculated by adding the prism-antenna offset to the prism position. The currently used position rate is 10 Hz with an accuracy of 0.01 s. As the vendor provides and API for the MS60 system this values will be improved for future measurements.

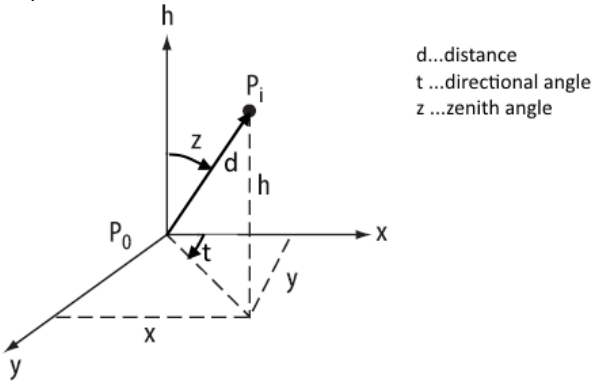

Figure 4: Determination of the (x,y,z) coordinates using angle and distance measurements.

UAV

As UAV the DJI drone S1000+ is used. The octocopter has a weight of 4.9kg and is able to carry a payload of approximately 6kg (including the battery). Fully equipped, the air time is approximately 15 minutes (compare Table 2). The S1000+ has an IMU, GPS and compass module on board for stabilization. However, as the payload generates and transmits GPS like signals, the flight mode with deactivated GPS module was chosen due to safety reasons. Despite the fact that the GPS module is able to track the real GPS signals, due to the used shifted carrier frequency, we have not enough experience to eliminate the possibility of disturbances yet. To attach the different devices at the drone, special constructed and 3D printed plastic mounts are used. A list with used devices, mounts with corresponding weights are shown in Table 2.

Table 2: UAV item list with weight analysis

ITEM	WEIGHT [g]
DJI S1000+	4891
Drone Battery Pack	1985
Battery Pack Mount	78
USRP Battery Pack	408
USRP 2950R	1885
USRP Mount	80
HELIX Antenna	12
Antenna Mount	56
Mini 360° Prism	26
Prism mount	31
TOTAL	9452

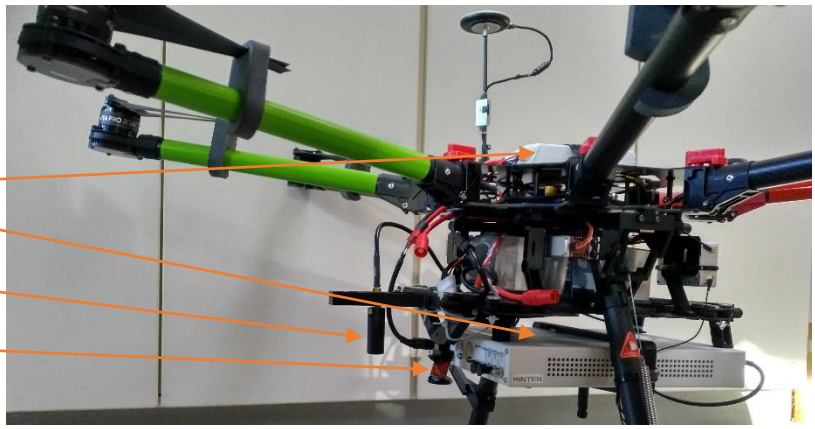

Figure 5: Fully equipped drone as used in the test scenarios.

RESULTS

In this section, two measuring campaigns are presented. First a measurement with only one antenna is discussed. In this test the usability of the component composition was tested. With a single antenna no pseudorange difference could be calculated, however, the drone movements can be monitored by a Doppler shift analyses. The results are plotted in Figure 6, Figure 7 and Figure 8. The 300 second recording can be divided into three segments.

In the first segment, from 0 to 70 seconds, the signal is acquired and the drone hovers at a height of 20 m at a stationary position (1-2 m drift). The second segment is from 70 to 200 seconds, where the drone approaches and departs from the antenna position. This movements with the corresponding speed is clearly visible in the Doppler shift plot in Figure 6 (bottom).

The C/N0 drop between 160 to 195 seconds in Figure 8 is due to a tree in the line of sight. In this situation a larger error in the DLL, PLL and FLL (Figure 7) is also visible. In the third segment, 200 to 300 seconds, the drone is again hovering at a stationary position (1-2 m drift) and is landing at the end. The landing is visible due to a signal power drop and greater errors after 250 s.

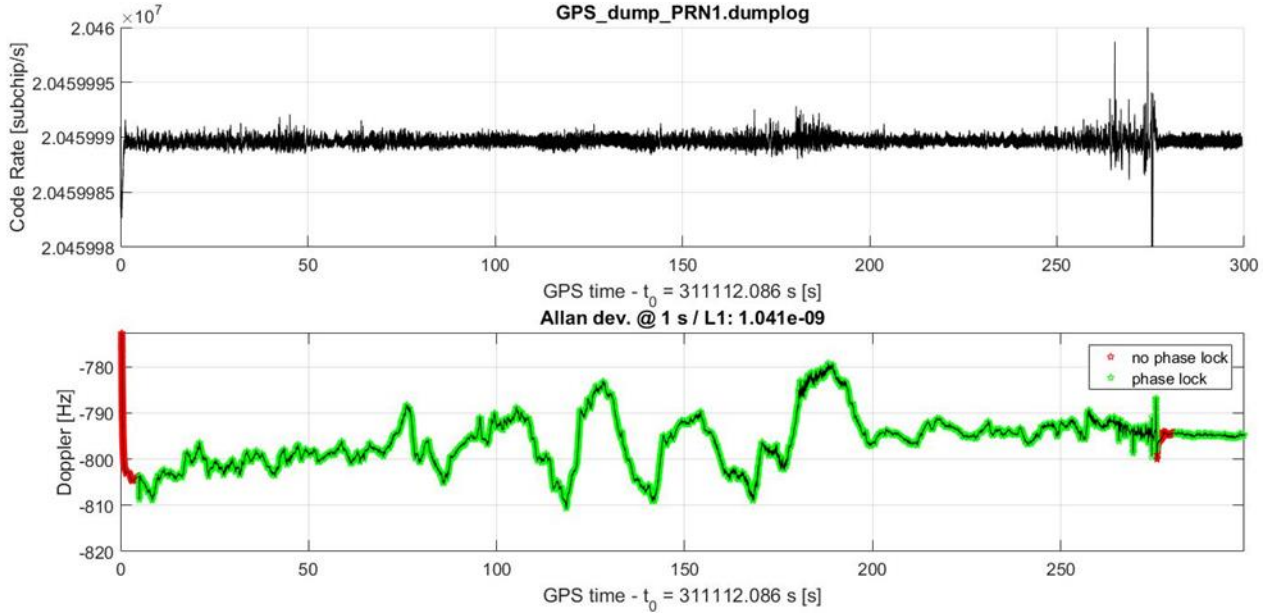

Figure 6: Single antenna analysis with the code rate (top) and the Doppler shift (bottom).

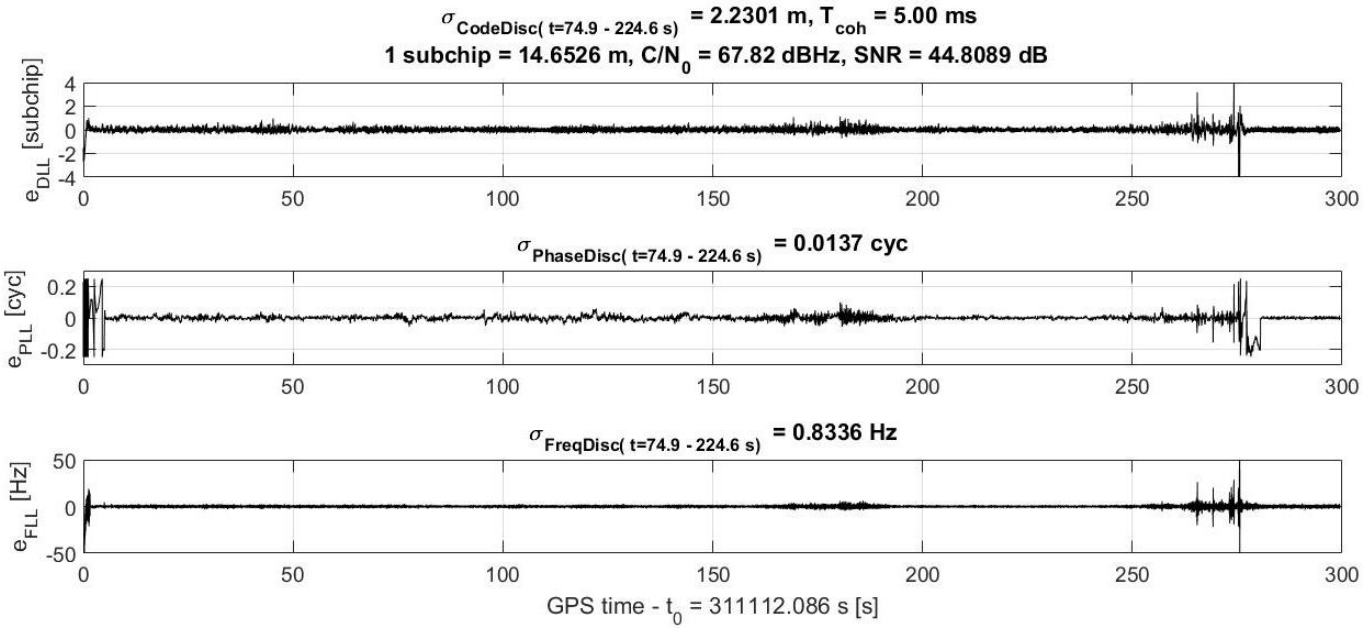

Figure 7: Error of Daly Lock Loop (DLL) Top, Phase Lock Loop (PLL) Middle and Frequency Lock Loop (FLL) Bottom.

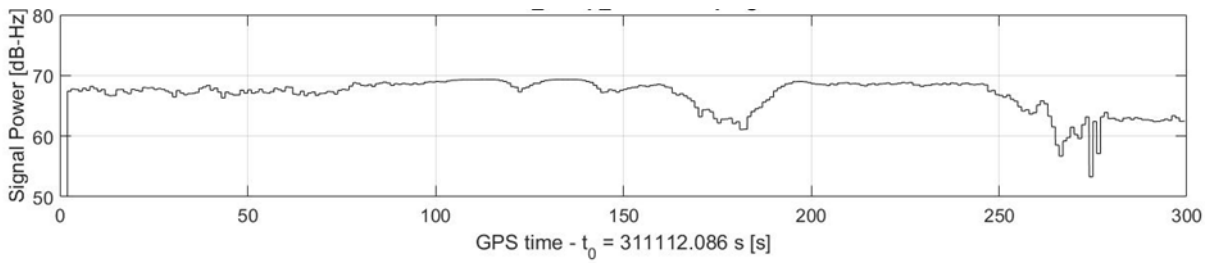

Figure 8: Signal Power (C/N0) of the single antenna analysis.

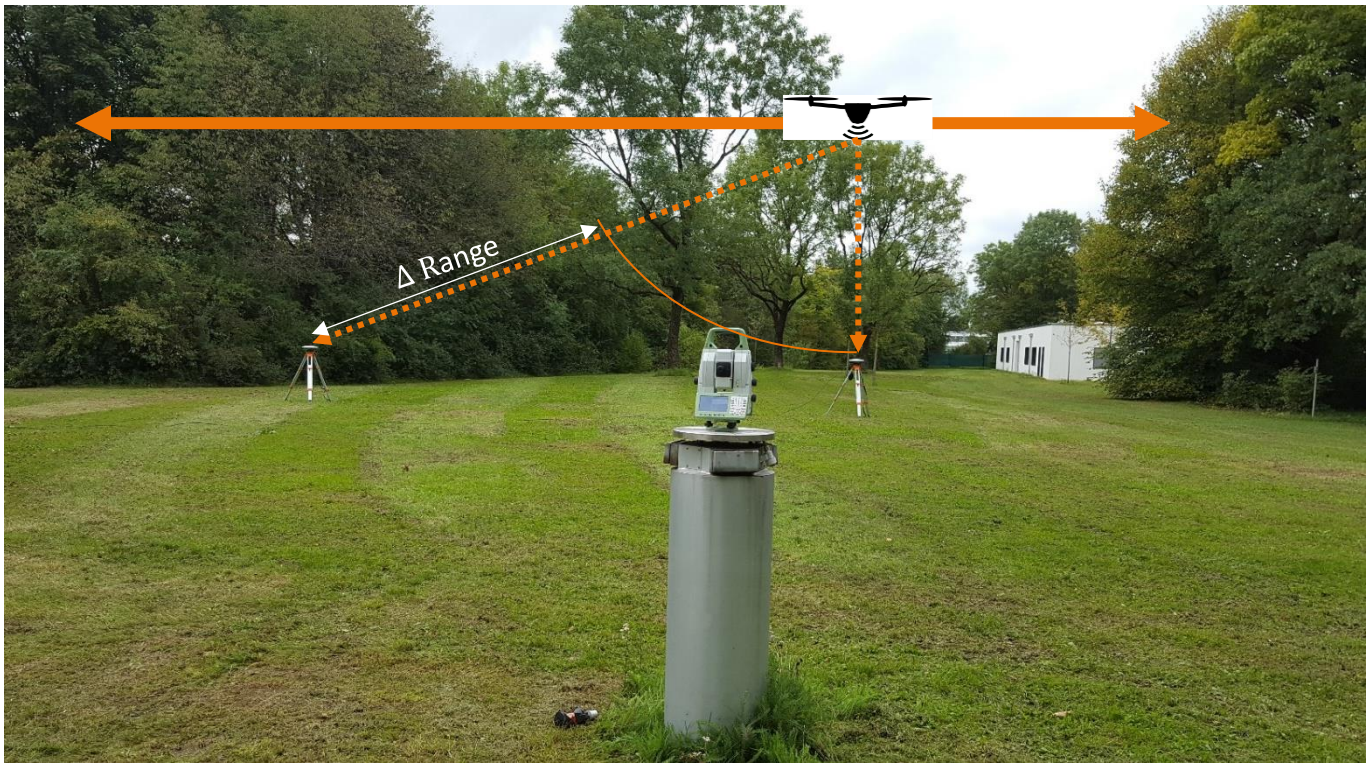

Figure 9: Setup of two antenna measurement.

The second measuring campaign realizes the basic concept with two synchronized antennas. In this campaign the drone flies approximately 4 m above the antennas. The movement is from right to left and back, along the connection line of the antennas, compare Figure 9. In Figure 10 the computed pseudorange differences for code and phase measurement is plotted. Both measurements show the expected behavior, the difference increases when the drone flies from right to left and decreases on the way back. The Code pseudorange measurement show, however, a large (~ 2 m amplitude) oscillation around the expected behavior. This oscillation seems to be very regular and indicates a systematic failure in the system. Further inspection into this has to be done. In contrast, the phase pseudorange shows a smooth and well behavior. Therefore, just the phase pseudorange difference was compared with the geometrical distance difference (Figure 11, top). The phase PR was therefore shifted in X (time) and Y (distance) direction. The X direction shift was calculated via cross correlation of the graphs. This step is necessary, as this early setup has not synchronization between receive antennas and tacheometer. In future this sync, will be established however. The Y direction shift was determined with a minimization of the RMSE of the difference of both graphs. The resulting standard deviation is $\sigma_{std} = 0.068$ m. The plotted difference is shown in Figure 11 (bottom).

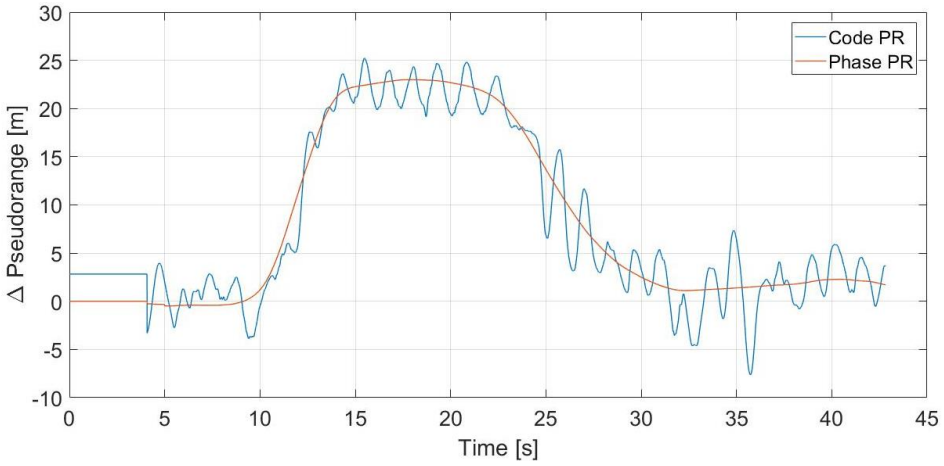

Figure 10: Pseudorange difference for Code and Phase measurement.

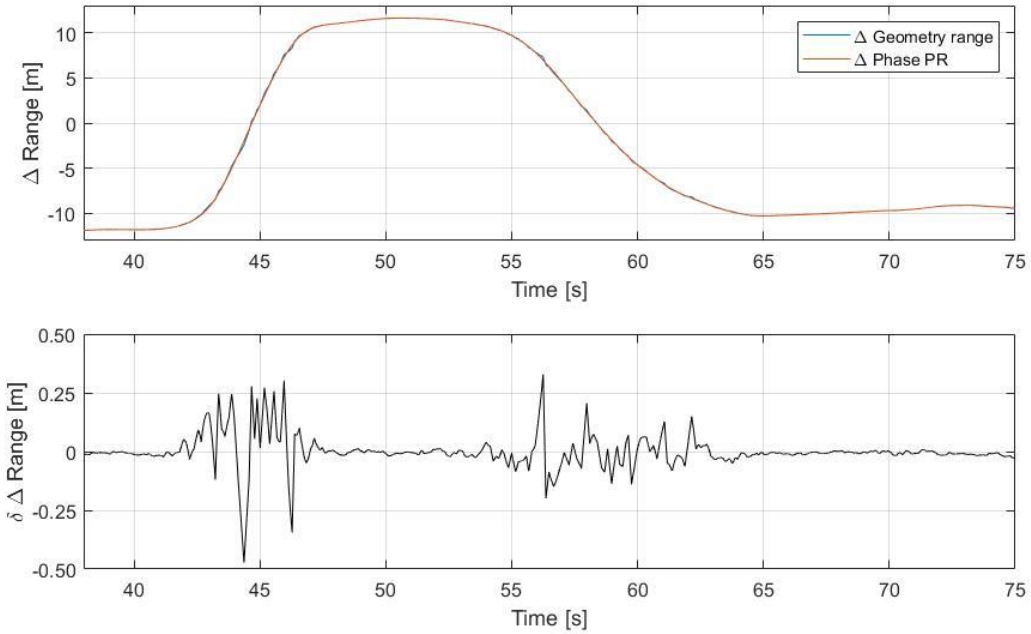

Figure 11: Phase PR difference compared with the geometrical difference. On the top both differences are plotted. The Bottom graphs shows the difference of the top graphs. The resulting standard deviation is $\sigma_{std} = 0.068\ m$.

CONCLUSIONS AND OUTLOOK

It was shown that it is feasible to use UAV's as GNSS satellites. The USRP 2950R can be used for the GNSS signal generation. The internal OCXO time stability is sufficient and the FPGA programmed with LabVIEW can be used to generate the GNSS signal. A procedure was presented to use the USRP in a standalone mode. The GNSS signal was transmitting from the flying drone and was received and recorded by single and multiple antennas. The recorded signals were analyzed in terms of Doppler shift, Code rate, DLL, PLL, FLL and C/N_0. The approach to analyze the signal by using pseudorange differences in combination with measured geometrical range differences was presented and it was shown that it is a possible and potential technique to analyze error sources in the communication path.

The feasibility is shown, now the potential need to be explored. The source of the oscillation in the code pseudorange need to be clarified as well as the sensibility of the system. The future development steps include multiple and variable signals, time synchronized independent receivers, time synchronization of the positioning and ranging unit, drone hardware optimization and including additional threat scenarios regarding jamming and spoofing.

This system shows great potential in the wide field of signal analyzation and optimization be it in the field of multipath, robustness, performance, authentication or channel coding at existing or future signals and services.

REFERENCES

[1] National Instruments Corporation, "USRP RIO Software Defined Radio", URL:http://www.ni.com/datasheet/pdf/en/ds-538, 2014

[2] National Instruments Corporation, "SPECIFICATIONS USRP-2950", URL:http://www.ni.com/pdf/manuals/374194d.pdf, 2017

[3] National Instruments Corporation, "USRP-2920 Specifications", http://www.ni.com/documentation/en/software-defined-radio-device/latest/specs-usrp-2920/specs/, 2017

[4] Microsemi Corporation, "XPRO High-Performance Rubidium Oscillator", URL:https://www.microsemi.com/product-directory/embedded-clocks-frequency-references/3962-xpro, 2014

[5] IFEN, "SX3 GNSS Software Receiver", URL:http://www.ifen.com/products/sx3-gnss-software-receiver.html, 2017

[6] Leica Geosystems, "Leica Nova MS60 – The World's First Self-Learning MultiStation", URL: http://leica-geosystems.com/products/total-stations/multistation/leica-nova-ms60, 2017

[7] Leica Geosystems, "Reflectors", URL: http://leica-geosystems.com/products/total-stations/accessories/reflectors, 2017